International Journal of Advanced Engineering and Technology Research
ISSN: 3106-8677 (Print), ISSN: 3106-8685 (Online) | Vol. 1, No. 3, 2026

Development of a Lateral Flow Assays Sensing Platform Based on Aptamer-Modified Pt@Au Nanozymes for The Detection of Kanamycin

Guobin Xiong

Chongqing University of Technology, Chongqing 400054, China

Abstract: Thanks to its ease of use, speed, efficiency, and the ability to visually identify detection signals without the need for specialized equipment, lateral flow assay (LFA) technology has become a key analytical method in fields such as pharmaceutical safety testing and biomedicine. Traditional lateral flow assays use colloidal gold as a signal label; however, due to the limited intensity of its colorimetric signal, conventional LFA technology suffers from insufficient sensitivity and fails to meet det ection requirements. Based on this, this study synthesized platinum-based bimetallic nanozymes (Pt@Au). Through the synergistic interaction of multiple metal elements, these nanozymes exhibit high enzyme-like catalytic activity. They were then applied to lateral flow assay technology to enable sensitive detection in biosensing. The Pt@Au nanozyme possesses high peroxidase-like catalytic activity, enabling it to catalyze the color-forming substrate TMB within an extremely short time to amplify the signal and achieve sensitive color development. By using an aptamer as an intermediate competitive molecule, streptavidin was conjugated to biotin-DNA molecules on the surface of the Pt@Au nanozyme to competitively detect kanamycin in LFA test strips. The detection linear range is 100 ng/mL to 800 ng/mL. Within the spiked concentration range of 50 to 250 ng/mL, the recovery rates of this method range from 95.1% to 105.2%, with relative standard deviations (RSD) of 3.4% to 8.5%, providing a new technical approach for the rapid on-site detection of antibiotic residues.

Keywords: Lateral flow assay, platinum-based nanozyme, bimetallic nanozyme, kanamycin.

1. Introduction

Aminoglycoside antibiotics are a class of antibiotics that have long been used to treat bacterial infections. They possess a structure comprising an amino sugar and an amino cyclitol, and are characterized by good water solubility, stability, a broad spectrum of antimicrobial activity, potent antibacterial efficacy, and efficient absorption and excretion [1]. Kanamycin, as an aminoglycoside antibiotic, is widely used in the clinical treatment of infectious diseases and in veterinary medicine due to its low cost and ease of administration [2, 3]. However, excessive use of kanamycin can lead to its accumulation in the body, resulting in side effects such as kidney disease, ototoxicity and drug allergies [4-6]. This makes it necessary to monitor kanamycin concentrations. Currently, the detection of residual kanamycin concentrations primarily relies on methods such as high-performance liquid chromatography (HPLC), liquid chromatography-mass spectrometry (LC-MS) and fluorescence assays; most of these methods require large-scale equipment and specialist personnel [3, 7, 8]. Although traditional detection methods can accurately detect kanamycin, their limitations prevent convenient and rapid on-site testing, which causes inconvenience for ordinary households. Therefore, there is a need to establish a rapid, specific and simple method for the sensitive detection of kanamycin and other antibiotic residues.

Lateral flow chromatography technology has been widely adopted in the field of point-of-care testing due to its ease of use, low cost and visual results [9-11]. In traditional lateral flow chromatography assays, colloidal gold is used as a signal label because, as a precious metal, it offers advantages such as chemical stability and ease of surface modification [12]. However, colloidal gold also suffers from the drawbacks of insufficient sensitivity and inadequate colour development. Enzyme-mediated LFA test strips offer the advantages of sensitive colour development and simple operation. In recent years, nanozymes have become a research focus for signal amplification strategies due to their excellent catalytic activity, good stability and ease of functionalisation. [13] Among these, platinum-based nanozymes not only possess high catalytic activity but also benefit from the stability and ease of surface modification characteristic of precious metals, making them a strong alternative to colloidal gold. Currently, most lateral flow chromatography (LFA) techniques utilise antibodies as the biomolecular recognition elements for signal detection; however, antibodies suffer from long production cycles, poor stability and high costs. Furthermore, as kanamycin is a small molecule, antibodies have poor recognition capabilities for it, which limits the application of antibody-based LFA test strips [13]. Kyung-Mi Song et al. successfully screened for aptamers of kanamycin and its derivatives using an affinity chromatography-based SELEX system, and confirmed the interaction between the screened aptamers and kanamycin through Tm measurements and fluorescence binding assays [14]. As adaptors exist as single-stranded deoxyribonucleic acid (ssDNA) or ribonucleic acid (RNA), they offer the advantages of low cost, strong binding affinity for small molecules, and ease of preparation, thereby presenting an opportunity for the detection of kanamycin using lateral flow chromatography technology [15].

In this study, platinum-gold bimetallic nanozymes (Pt@Au) were synthesised, combining the excellent catalytic activity of PtNPs with the stability of AuNPs. Polyvinylpyrrolidone was incorporated during the synthesis process to impart colloidal properties to the Pt@Au in aqueous solution. The Pt@Au nanozyme exhibits high peroxidase-like catalytic activity, enabling signal amplification through the catalytic

conversion of the chromogenic substrate TMB within a very short time, thereby achieving sensitive colourimetric detection. By utilising an aptamer as an intermediate competitive molecule, streptavidin was conjugated to biotin-DNA molecules on the surface of the Pt@Au nanozyme, allowing for the competitive detection of kanamycin on LFA test strips. Through the synthesis, characterisation, evaluation of enzyme-like activity, and surface functionalisation of the Pt@Au nanozyme, the detection conditions were systematically optimised. A sensitive, highly specific, and stable method for the detection of kanamycin was established, and its performance in real-world samples was validated, providing a new technical approach for the rapid on-site detection of antibiotic residues.

2. Experimental Methods

2.1. Chemical and Materials

All chemical reagents used in this experiment were of analytical grade. Auric acid ($HAuCl_4 \cdot 3H_2O$), $H_2PtCl_6 \cdot 6H_2O$, sucrose, polyvinylpyrrolidone (PVP, MW 10 kDa), L-ascorbic acid (L-AA), Tween-20, oxytetracycline (OTC), tetracycline (TC), ciprofloxacin (CIP), gentamicin (GEN), streptomycin (STR), tobramycin (TOB) and 3,3',5,5'-Tetramethylbenzidine (TMB) were purchased from Aladdin Chemical Reagents (Shanghai) Co., Ltd. The DNA-biotin molecules were supplied by Shanghai GenScript Biotech Co., Ltd. The DNA sequences used are as follows:

Biotin-DNA1: Biotin-AAAAAAAAAATC GGCTTAGC
Biotin-DNA2: Biotin-AAAAAAACCCCCAACTC
Biotin-DNA3: Biotin-GCTAAGCCGATTTTTTT
Aptamer: TTTTGGGGGTTGAGGCTAAGCCGATTT

2.2. Instrument

The morphology and size of Pt@Au were characterised using a scanning electron microscope (SEM; Gemini 300, Zeiss, Germany) and a transmission electron microscope (TEM; JEOL JEM-F200, Japan). X-ray photoelectron spectroscopy (XPS) spectra of the material were measured using an X-ray photoelectron spectrometer (Thermo Scientific K-Alpha, USA). Fourier-transform infrared (FT-IR) spectra were obtained using a FI-IR infrared spectrometer from PerkinElmer. Ultraviolet-visible (UV-Vis) spectra were measured using a UV-2450 spectrophotometer from Unico. Test strips were prepared using a simple film-coating apparatus (Bofan Biotechnology Co., Ltd.).

2.3. Synthesis of Colloidal Gold

SeedsColloidal gold seeds are obtained by reducing chloroauric acid using trisodium citrate, as follows: All glassware is thoroughly washed with ultrapure water and dried; it is then soaked overnight in aqua regia (concentrated hydrochloric acid: concentrated nitric acid = 3:1), rinsed thoroughly with ultrapure water, dried, and set aside for use. Heat 100 mL of a 0.01% aqueous solution of chloroauric acid until boiling, then rapidly add 2 mL of a freshly prepared 1% aqueous solution of trisodium citrate whilst stirring vigorously. The solution rapidly turns a wine-red colour; continue boiling for 15 minutes, then cool and add ultrapure water to a final volume of 100 mL to obtain a colloidal gold solution, which is stored in a refrigerator at 4 °C. The seed concentration was determined by size analysis via transmission electron microscopy and the initial gold concentration.

2.4. Synthesis of Pt@Au materials

Pt@Au was synthesised via the reduction of chloroplatinic acid hydrate, following the method described by Gao et al[16]. In a typical synthesis, 31 μL (10 nM) of 15 nm gold seeds were mixed with 969 μL of ultrapure water, followed by the addition of 20 μL of 20 wt% polyvinylpyrrolidone. The solution was briefly vortexed and incubated for 5 minutes to allow the polymer to coat and stabilise the particles. L-ascorbic acid (40 μL, 100 mg/mL) was then added, followed by 40 μL of chloroplatinic acid hydrate (100 mM). After mixing, the mixture was immediately incubated at 65 °C for 30 minutes until the solution changed colour from red to dark brown, indicating successful platinum deposition onto the gold seeds. Subsequently, wash three times consecutively with ultrapure water at 9000 rpm, resuspend to 1 mL, and store at 4 °C.

2.5. Preparation of Pt@Au Conjugates

2.5.1. Pt@Au-modified SA

Functionalisation was carried out by mixing 500 μL of Pt@Au (500 pM), 50 μL of phosphate-buffered saline (PBS, 50 mM, pH 6.4) and 20 μL of SA (1 mg/mL). The mixture was shaken at room temperature for 3 hours. Subsequently, 100 μL of BSA (1 mg/mL) was added to the mixture. The mixture was then shaken at room temperature for a further hour. The mixture was then washed three times consecutively with ultrapure water at 9000 rpm to remove excess residual reagents. The product was resuspended in PBST to yield a final volume of 500 μL of Pt@Au-SA (500 pM).

2.5.2. Pt@Au-SA-modified DNA

Mix 500 μL of Pt@Au-SA solution with 5 μL of Biotin-DNA1 solution (10 nM). After shaking for 1 hour, wash three times with PBST solution at 7000 rpm, then resuspend to a final volume of 500 μL to obtain the Pt@Au-SA-DNA complex.

2.6. Evaluation of the Catalytic Activity of Pt@Au-type Enzymes

To determine the peroxidase-like activity of the nanozyme, 5 μL of Pt@Au solution (500 μM), 10 μL of hydrogen peroxide (10 mM) and 20 μL of TMB (10 mM) were added to 840 μL of acetic acid buffer (0.01 M, pH 4). The final solution was analysed at 653 nm using a UV-Vis spectrophotometer.

2.7. Manufacture of Lateral Flow Assay Strips

Lateral flow assay strips (LFA strips) consist of four components: an absorbent pad, an NC membrane, a sample pad and a backing sheet. They are used to detect kanamycin. Biotin-DNA2 is applied to the NC membrane to form the test line (T line), whilst Biotin-DNA3 is applied to the NC membrane to form the control line (C line). The NC membrane is then dried at 37 °C for 2 hours. Finally, the sample pad, NC membrane and absorbent pad are laminated onto the backing sheet, with an overlap of approximately 2 mm between each component, and cut into strips 3 mm wide. The prepared LFA strips are packaged in desiccant-filled pouches and stored at room temperature for use.

2.8. Lateral Flow Assay Detection of Kanamycin

To validate the feasibility of the cascade LFA, 10 μL of kanamycin aptamer solution (10 nM) was mixed with 10 μL

of kanamycin solution (at various concentrations), incubated at room temperature for 30 minutes, and then mixed with 30 μL of PBST buffer. Subsequently, the mixed solution was dispensed into a 96-well plate, and the sample pad end of the LFA strip was inserted into the well. After 10 minutes, the colourimetric results were observed visually and recorded using a smartphone. To amplify the signal, 20 μL of chromogenic substrate solution was dispensed onto the LFA test strip. After 5 minutes, the colourimetric results were observed visually and recorded using a smartphone. The final images were processed and analysed using ImageJ.

3. Results and Discussion

3.1. Characterizations of Pt@Au Nanomaterials

The synthesis of Pt@Au nanozymes is shown in Fig. 1a. Following a method reported in the literature, platinum nanozyme particles were synthesized by reducing chloroauric acid to deposit it onto gold seeds [16]. At the beginning of the synthesis, PVP was used to coat the colloidal gold seeds to ensure the colloidal stability of the resulting particles and to minimize contamination when exposed to complex media during LFA [17]. Analysis of the synthesized Pt@Au using a UV spectrophotometer revealed, as shown in Fig. 1b, that the Pt@Au exhibits a broad absorption peak and the particles are black in color, with the aqueous solution displaying colloidal properties. Measurement of the hydrated particle size of the Pt@Au using a particle size analyzer, as shown in Fig. 1c, indicated that the hydrated particle size ranges between 140 and 180 nm, which meets the requirements for signal molecules in LFA experiments [18].

X-ray photoelectron spectroscopy (XPS) was employed to further characterize the electronic interactions of the Pt@Au nanozyme. The full-scan results in Fig. 1d show that, within the binding energy range of 0–1200 eV, the sample exhibits characteristic signal peaks for three elements: C 1s, Pt 4f, and Au 4f. Peak fitting of the high-resolution XPS spectrum for the Pt 4f orbital (Fig. 1e) yields two sets of characteristic peaks corresponding to the spin-orbit splitting of the Pt 4f orbital: the Pt $4f_{5/2}$ and Pt $4f_{7/2}$ orbital signals. Among these, the Pt $4f_{7/2}$ peak at 71.2 eV ₂ peak at 71.2 eV and the Pt $4f_{5/2}$ peak at 74.5 eV are attributed to zero-valent metallic platinum (Pt^0); the Pt $4f_{7/2}$ peak at 72.6 eV and the Pt $4f_{5/2}$ peak at 75.9 eV are attributed to divalent oxidized platinum (Pt^{2+}) [19]. The results indicate that Pt in the Pt@Au nanozyme primarily exists in the reduced metallic form Pt^0, with only a small amount of the oxidized form Pt^{2+}, confirming that the Pt precursor was successfully reduced during the synthesis process. Quantitative calculations based on the peak areas of the characteristic XPS peaks yielded the relative elemental composition on the surface of the Pt@Au nanozyme (Fig. 1f): the relative content of C was 87.2%, that of Pt was 12.6%, and that of Au was only 0.2%, which is attributed to the use of a low-concentration gold seed as the growth carrier during the synthesis.

Characterization of the Pt@Au nanozyme via TEM and SEM (Fig. 2a–b) revealed a spherical morphology with excellent dispersion, and an average particle size of approximately 150 nm. High-resolution transmission electron microscopy (HRTEM) images (Fig. 2c) reveal continuous and ordered lattice fringes, indicating that the synthesized Pt@Au nanozymes possess good crystallinity; The lattice spacing of 0.22 nm closely matches the standard lattice spacing of the (111) crystal plane in face-centered cubic (fcc) metallic Pt [16]. The EDS elemental mapping results (Fig. 2d–f) clearly show the distribution of Pt and Au elements within the material, confirming the synthesis of the bimetallic nanozyme.

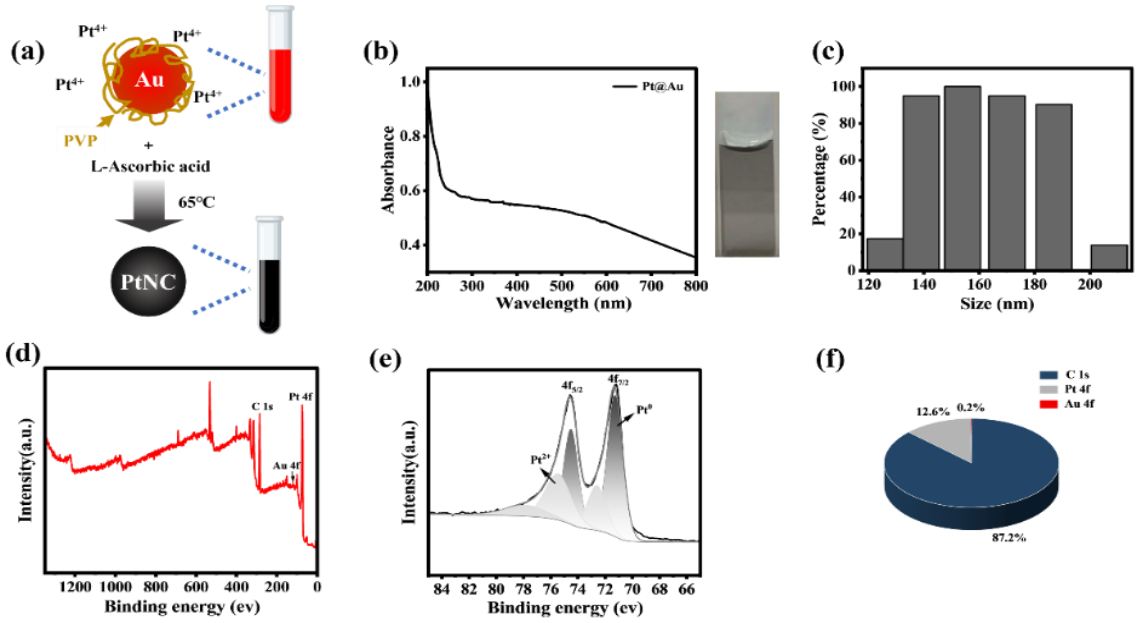

Figure 1. (a) Schematic Diagram of Pt@Au Synthesis; (b) UV-Vis absorption spectrum of Pt@Au nanozymes; (c) Hydrated particle size distribution of Pt@Au nanozymes; (d) Full XPS spectrum of Pt@Au nanozyme; (e) High-resolution Pt 4f spectrum; (f) Pie chart of relative surface elemental content

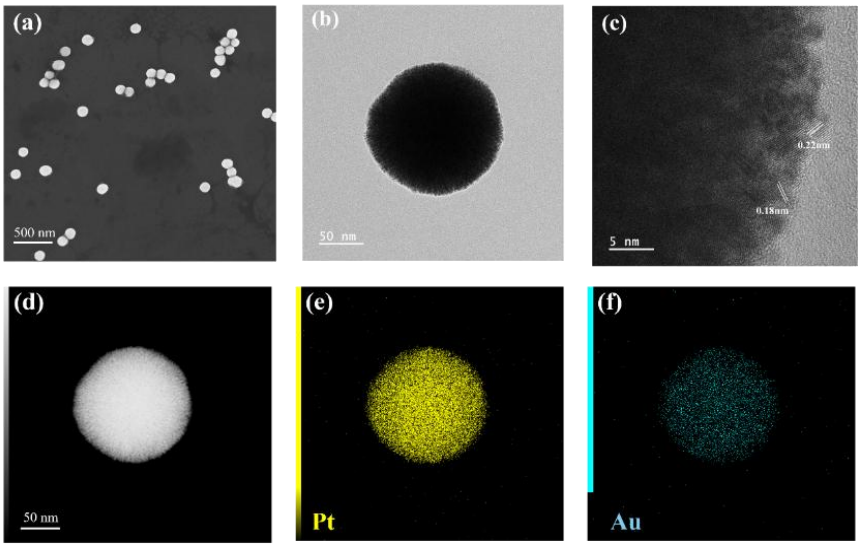

Figure 2. Morphology and Elemental Distribution Characterisation of Pt@Au Nanozymes: (a) SEM image; (b)TEM image; (c) HRTEM image; (d) STEM bright-field image; (e) (f) Elemental EDS distribution

3.2. Investigation of Oxidase-like Activity of the Pt@Au

The validation results for peroxidase-like activity are shown in Fig. 3a. A strong characteristic absorption peak of oxidized TMB was observed at 652 nm only in the reaction system containing the Pt@Au nanozyme, TMB substrate, and H_2O_2; whereas the Pt@Au+TMB control group without H_2O_2 and the TMB+H_2O_2 control group without the nanozyme showed no significant characteristic absorption signals. These results confirm that the Pt@Au nanozyme possesses peroxidase-like catalytic activity, capable of generating a significant colorimetric signal by catalyzing the oxidation of TMB by H_2O_2, thereby providing the conditions for signal amplification in the lateral flow chromatographic detection system. To evaluate the optimal chromogenic substrate for the nanozyme, the catalytic activity of the Pt@Au nanozyme toward three commonly used chromogenic substrates—TMB, o-phenylenediamine (OPD), and 2,2'-azobis (3-ethylbenzothiazole-6-sulfonic acid) (ABTS)—was compared, with the results shown in Fig. 3b. Under identical reaction conditions, only the TMB substrate system exhibited a very strong characteristic absorption peak, while the OPD and ABTS reaction systems showed no obvious color development signal; therefore, TMB was selected as the color development substrate for subsequent experiments. Furthermore, Pt@Au exhibited the highest peroxidase-like activity at pH = 4 (Fig. 3c).

To quantify the peroxidase-like catalytic activity of the Pt@Au nanozyme, steady-state kinetic studies of the Pt@Au-H_2O_2-TMB system were conducted to determine the steady-state kinetic parameters Km and Vmax. Linear fitting of the data was performed using the Lineweaver-Burk double-reciprocal model (Fig. 3e–f), yielding a Michaelis constant K_m = 0.167 mM and a maximum reaction rate V_{max} = 77.8 × 10^{-7} M/s for the Pt@Au nanozyme with TMB as the substrate; when H_2O_2 was used as the substrate, the Michaelis constant K_m was 1.41 mM, and the maximum reaction rate V_{max} was 41.71 × 10^{-7} M/s. The K_m value of the Pt@Au nanozyme for TMB is significantly lower than that of native HRP and Fe_3O_4 nanozymes, indicating that this nanozyme possesses stronger specific binding capacity for TMB, the chromogenic substrate in the lateral flow immunoassay system, and can initiate highly efficient catalytic color development reactions even under low TMB concentration conditions [20, 21].

The stability of the Pt@Au nanozyme is of critical importance. As shown in Fig. 3d, the material maintains good catalytic activity over a wide temperature range of 4 °C to 65 °C; at room temperature (25 °C), it retains more than 85% of its relative catalytic activity. As shown in Fig. 4, after continuous storage at room temperature for 30 days, the relative catalytic activity of Pt@Au remains above 95%. Furthermore, during the 30-day storage period, the hydrated particle size of the Pt@Au nanozyme exhibited only a slight, gradual increase, and the PDI remained consistently below 0.3; a PDI of less than 0.3 is a criterion for excellent monodispersity of nanoparticles [22]. These results fully confirm that the prepared Pt@Au nanozyme possesses excellent long-term storage stability.

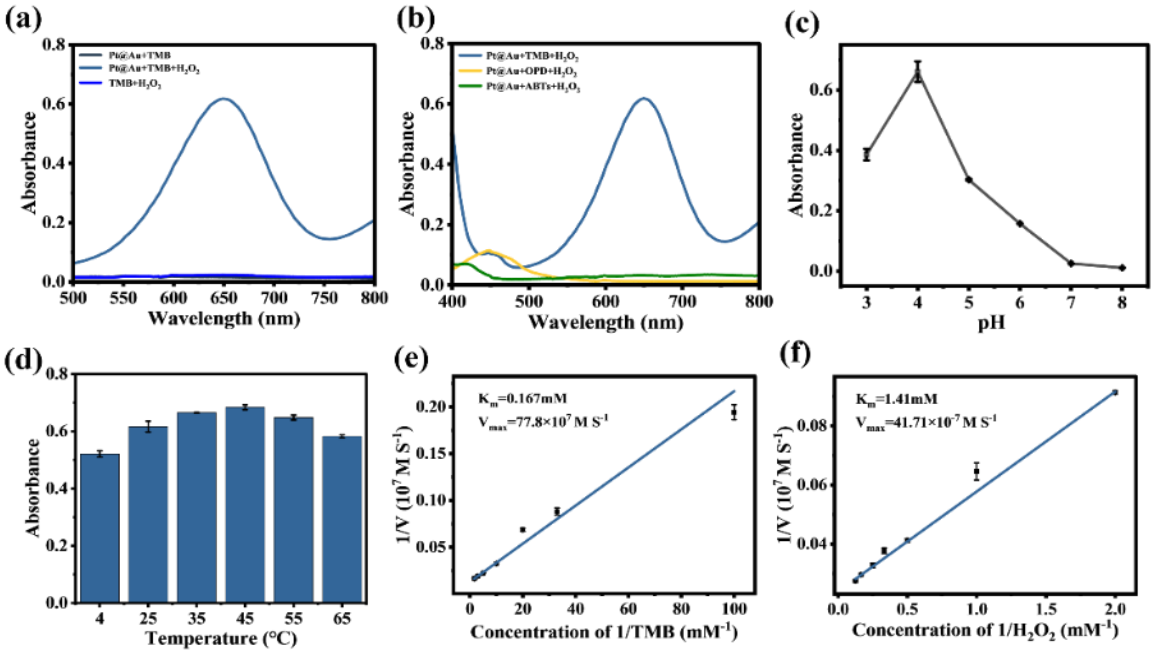

Figure 3. (a) UV absorption spectra of different systems; (b) Comparison of catalytic activity toward different substrates; (c) Effect of pH on catalytic activity; (d) Effect of temperature on catalytic activity; (e) Double reciprocal fitting curve with TMB as substrate; (f) Double reciprocal fitting curve with H_2O_2 as substrate.

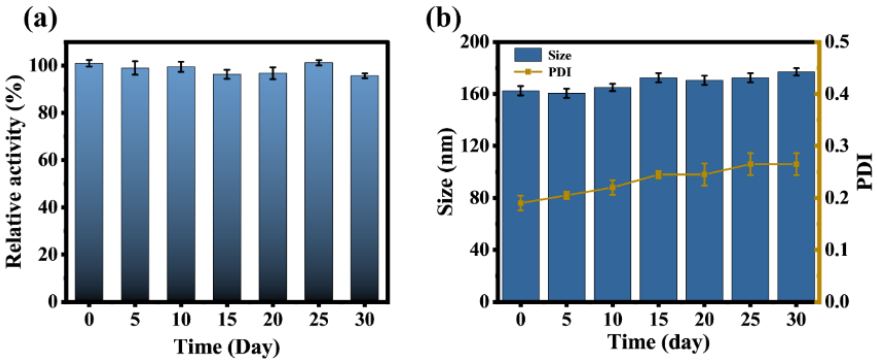

Figure 4. (a) Long-term catalytic activity stability of Pt@Au nanozymes; (b) Changes in hydrated particle size and PDI during storage

3.3. Modification and Characterization of Pt@Au

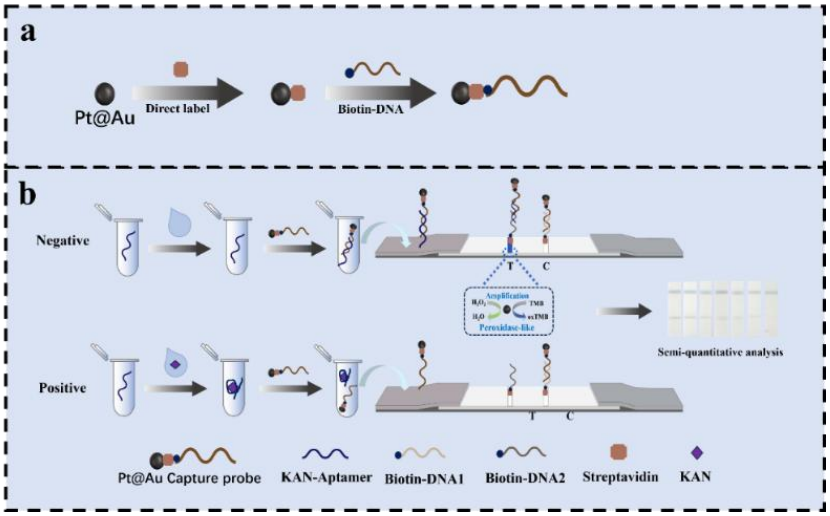

Figure 5. (a) Schematic diagram of the preparation process for Pt@Au-SA@DNA signal probes; (b) Schematic diagram of LFA for detecting kanamycin.

This study employs an aptamer-competitive detection scheme for the small-molecule compound kanamycin. Figure 5a illustrates the preparation process of the signal probe for the detection system. To immobilize the target DNA molecule

on the surface of the Pt@Au nanozyme, streptavidin (SA) was used to modify the material surface via electrostatic adsorption. Subsequently, a biotin-modified DNA molecule was directly linked to the Pt@Au-SA through the specific affinity between SA and biotin. Fig. 5b illustrates the principle of kanamycin detection: by modifying the Pt@Au nanozyme with SA, it binds to the complementary DNA strand of the biotin-modified kanamycin aptamer, forming a detection probe for the sensitive detection of the kanamycin aptamer and, consequently, the indirect detection of kanamycin.

To verify the successful construction of the signal-capturing probe, TEM was used to characterize the Pt@Au materials before and after modification. The unmodified Pt@Au nanozyme (Fig. 6a) exhibited a spherical morphology; the Pt@Au-SA@DNA capture probe (Fig. 6b) retained its intact spherical morphology, with no significant change in particle size but a distinct protein network structure on the surface, likely due to protein denaturation caused by the temperature during TEM imaging [23]. Changes in the zeta potential serve as direct evidence of successful surface modification of the nanomaterial. The results show (Fig. 6c) that the zeta potential of the Pt@Au nanozyme is −43.2 mV; after SA modification, the absolute value of the zeta potential of Pt@Au-SA decreased significantly to −25.6 mV; following further conjugation with biotinylated DNA, the zeta potential of Pt@Au-SA@DNA became −33.4 mV. This is because the phosphate backbone of the DNA molecule carries a strong negative charge; successful conjugation significantly increased the negative charge density on the nanoparticle surface [24]. The aforementioned changes in potential confirm the successful synthesis of the signaling molecule. UV-Vis spectroscopy provided direct spectroscopic evidence for the successful modification of SA and DNA through changes in characteristic absorption peaks. The results show (Fig. 6d) that the Pt@Au nanozyme exhibits no distinct characteristic absorption peaks within the 200–800 nm scanning range; after SA modification, Pt@Au-SA exhibits a distinct characteristic absorption peak at 280 nm, which is a hallmark signal of protein molecules [25]; following further conjugation with biotinylated DNA, a characteristic absorption peak of nucleic acids appears at 260 nm [26]. The sequential appearance of these characteristic peaks fully confirms that both SA and DNA were successfully modified onto the surface of the Pt@Au nanozyme, indicating the successful construction of the signal-capturing probe. FT-IR spectroscopy further verified the success of the modification process at the molecular level through changes in the vibrational peaks of characteristic functional groups. The results show (Fig. 6e) that, compared to the Pt@Au nanozyme, both Pt@Au-SA and Pt@Au-SA@DNA exhibited characteristic infrared vibrational peaks of proteins: the strong peak at 1650 cm^{-1} corresponds to the amide I band (C=O stretching vibration of the peptide bond), and the characteristic peak at 1540 cm^{-1} corresponds to the amide II band (coupled N-H bending and C-N stretching vibrations) [27]. These characteristic peaks are signature signals of the streptavidin amine group, further confirming that SA has successfully bound to the surface of the Pt@Au nanozyme.

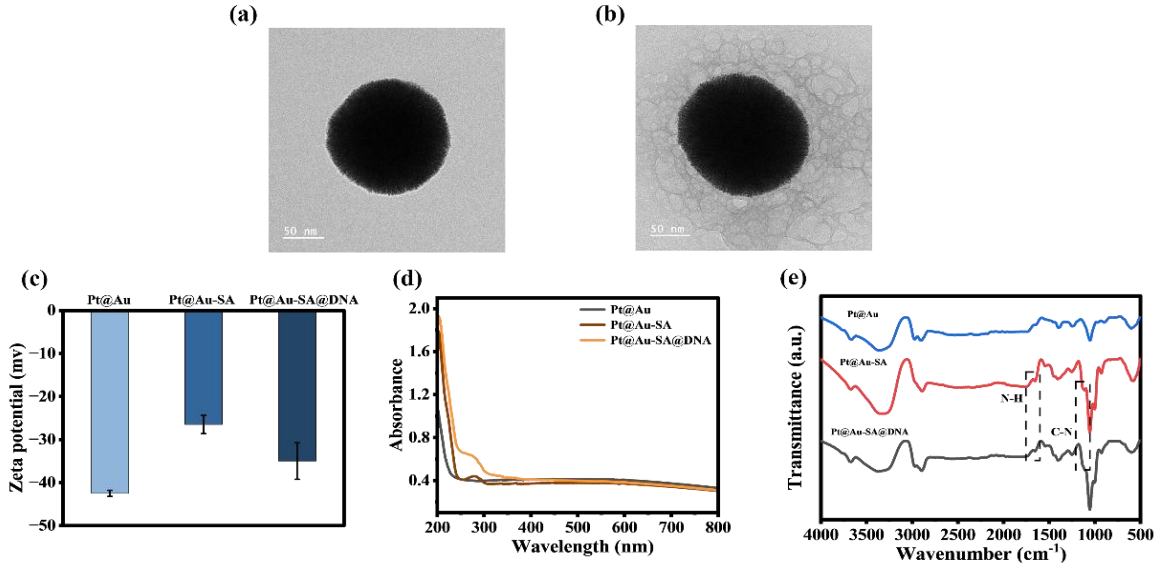

Figure 6. (a) TEM image of Pt@Au; (b) TEM image of Pt@Au-SA@DNA; (c) Zeta potential variation before and after modification; (d) UV-visible absorption spectrum; (e) FT-IR spectrum

3.4. Optimization of Conditions for Lateral Flow Assays

To establish a highly sensitive and color-stable lateral flow chromatographic detection system using Pt@Au nanozyme-based assays, this study systematically optimized the key operating parameters of the detection system, using the mean gray values of the test line (T zone) and control line (C zone) on the test strip as evaluation criteria. SSC (Saline-Sodium Citrate) buffer serves as the operating environment for maintaining nucleic acid binding activity, and its concentration directly affects the stability of the complex and the efficiency of the chromatographic detection. As shown in Fig. 7a, as the SSC buffer concentration increased from 1× to 8×, the gray values of both the T line and the C line exhibited a trend of initially rising and then stabilizing; therefore, 8× was selected as the optimal SSC buffer concentration. Chromatography time reflects the overall detection efficiency of the test strip. As shown in Fig. 7b, within the 0–10 min range, the gray scale values of both the T line and C line continued to increase with prolonged chromatography time. After 5 min, the signal reached saturation, indicating that the chromatography system had reached reaction equilibrium; further prolonging the time would not significantly enhance signal intensity, thus 5 min was determined to be the optimal chromatography time. Tween-20, a nonionic surfactant, is commonly used in lateral flow chromatographic systems to reduce nonspecific adsorption. As shown in Fig. 7c, 0.1% was

selected as the optimal Tween-20 concentration to ensure the system's specificity. The signal-capturing probe serves as the signal source for the entire detection system, and its volume directly determines the color saturation of the T-line. As shown in Fig. 7d, as the probe volume increased from 2 μL to 10 μL, the gray value of the T-line rose and stabilized at 8 μL; thus, 8 μL was determined to be the optimal probe volume.

The specific binding of the aptamer to kanamycin is a critical reaction step in competitive lateral flow assays; its binding efficiency determines the adequacy of the competitive reaction and the final detection sensitivity of the assay system. Further optimization of the assay conditions revealed, as shown in Fig. 8a, that an aptamer concentration of 10 nM ensures a clearly distinguishable color intensity in the negative control T-line while maximizing the color signal difference induced by target binding, making it the optimal working concentration for the competitive reaction. The specific binding of the aptamer to the target depends on the complementary matching of the secondary conformation of nucleic acids; the incubation temperature directly affects the conformational stability of the aptamer and the binding efficiency of the target-aptamer complex, thereby determining the adequacy of the competitive reaction. As shown in Fig. 8b, within the tested temperature range of 4 °C to 45 °C, the color intensity of the T line becomes lighter as the temperature increases, though the change is not significant. Considering the simplicity of lateral flow immunoassay detection, room temperature was selected as the incubation temperature. The incubation time directly determines the extent to which the target and aptamer specifically bind. As shown in Fig. 8c, the gray value of the T line reached its lowest point at an incubation time of 30 min; extending the incubation time further to 40 min did not result in a significant decrease in the gray value of the T line, indicating that the binding reaction between the target and the aptamer had reached equilibrium at 30 min, and the competitive reaction had proceeded fully.

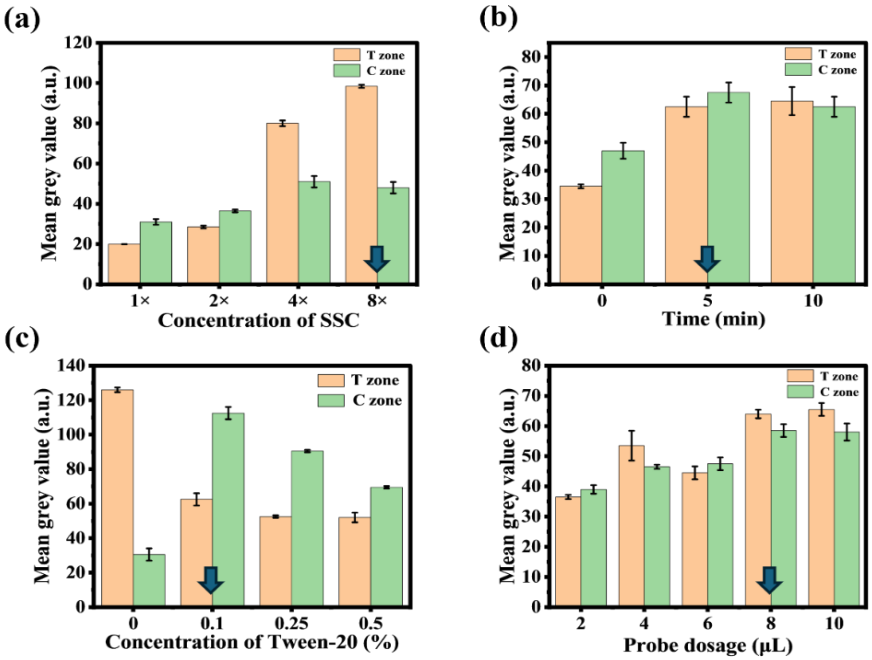

Figure 7. Optimization of Key Parameters in the Detection System: (a) SSC buffer concentration; (b) Chromatography time; (c) Tween-20 concentration; (d) Probe dosage

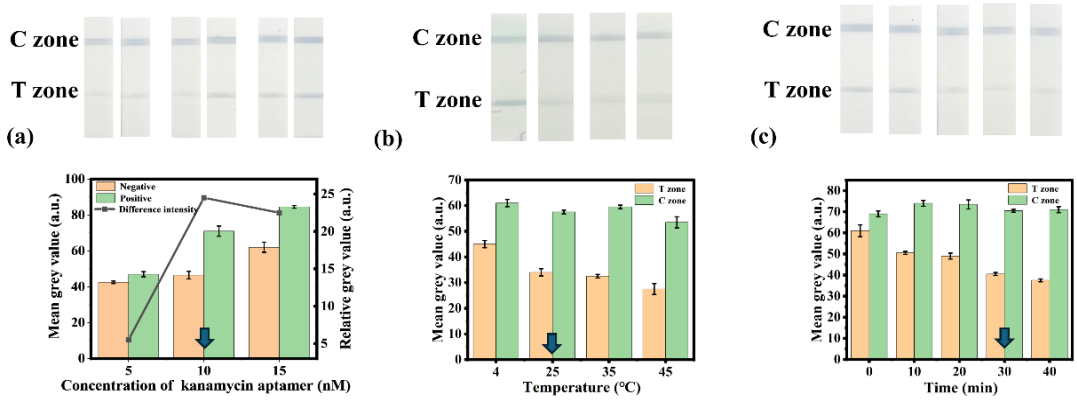

Figure 8. Optimization of aptamer binding conditions: (a) Aptamer concentration; (b) Incubation temperature; (c) Incubation time

3.5. LFA Assay for Kanamycin

Under the optimal reaction conditions described above, kanamycin was detected using the signal amplification provided by the TMB chromogenic substrate. The results shown in Fig. 9a depict photographs of the test strips after detection of kanamycin standards at different concentrations and subsequent addition of the TMB chromogenic substrate; kanamycin concentrations increase from left to right. Using ImageJ software, the average grayscale values of the T-line

were quantitatively measured after detection of kanamycin at different concentrations to establish a quantitative relationship between the detection signal and the target concentration. As shown in Fig. 9c, the average grayscale value of the T-line exhibits a significant negative correlation with kanamycin concentration. Within the concentration range of 0–1000 ng/mL, the grayscale value decreases continuously as the kanamycin concentration increases. After performing a logarithmic fit on the detection signals, a standard curve for this system was obtained (inset in Fig. 9c): Within the concentration range of 100 ng/mL to 800 ng/mL, the average gray value of the T-line exhibited a linear correlation with the logarithm of kanamycin concentration (LogcKAN). The linear regression equation was $y = -22.73x + 97.79$, with a coefficient of determination (R^2) of 0.98. The limit of detection was calculated to be 45.7 ng/mL. This indicates that the method possesses good quantitative detection capabilities.

Specificity is a key indicator for evaluating the practical value of lateral flow immunoassay methods. To verify the detection specificity of the Pt@Au nanozyme-based lateral flow immunoassay system developed in this study for kanamycin, a series of antibiotics at concentrations 10 times that of kanamycin were tested, using PBS buffer solution as the blank control. The results (Fig. 9b, d) showed that the T-line for the target compound, kanamycin, almost completely disappeared; for all interferent groups (OTC, TC, CIP, GEN, STR, TOB), the T-lines exhibited strong color bands similar to those in the blank group, with no visually detectable attenuation of color. This validated the specificity of the method.

Spiked recovery experiments were conducted on verified blank milk samples. The results (Table 1) showed that within the spiked concentration range of 50–250 ng/mL, the recovery rates of this method ranged from 95.1% to 105.2%, with relative standard deviations (RSD) ranging from 3.4% to 8.5%. These results indicate that this method exhibits excellent detection accuracy and reproducibility in the complex matrix of milk.

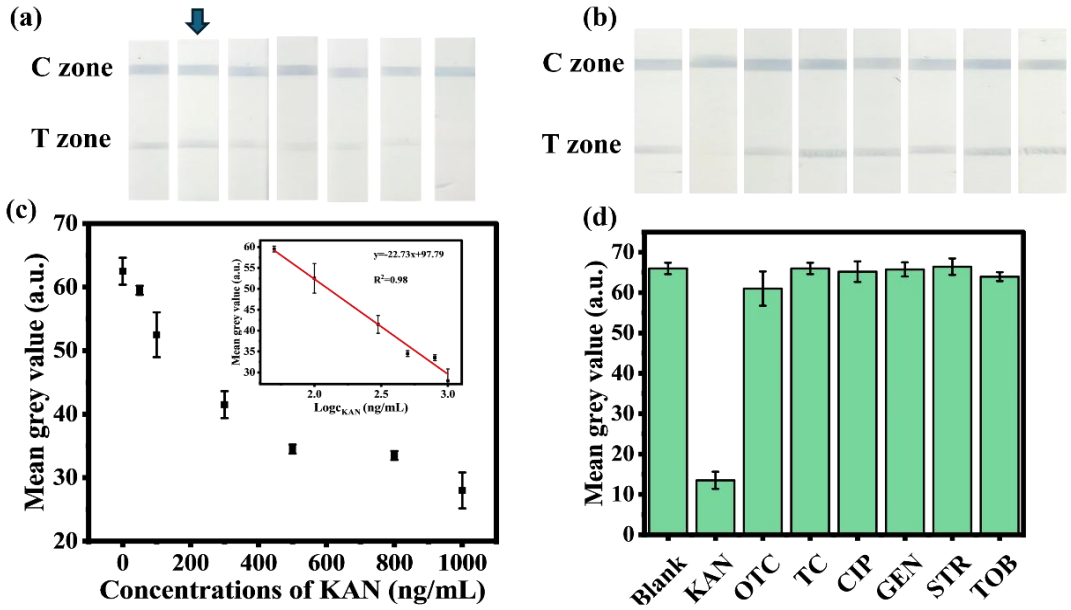

Figure 9. (a) (c) Photographs of color development and quantitative analysis of gray values for test strips at different concentrations of kanamycin (embedded figure shows linear fitting curve); (b) (d)Specificity Validation of Detection System: Photographs of Test Strip Color Development and Quantitative Analysis of T-Line Gray Scale Values

Table 1. Spiked Recovery Experiment for Kanamycin Concentration in Milk Samples (n=3)

Actual concentration (ng/mL)	Detection concentration (ng/mL)	Recovery (%)	RSD (%)
50	52.6	105.2	3.4
125	115.1	95.1	8.5
250	245.6	98.2	4.2

4. Conclusion

In summary, this chapter describes the synthesis of Pt@Au bimetallic nanozymes, which exhibit excellent peroxidase-like activity and suitable morphology and size. These nanozymes were applied to a lateral flow chromatographic platform by modifying them with DNA detection molecules. Using an aptamer as an intermediate, kanamycin was detected competitively, and signal amplification was achieved by adding the chromogenic substrate TMB. The assay achieved a detection range of 100 ng/mL to 800 ng/mL. Within the spiked concentration range of 50 to 250 ng/mL, the recovery rates ranged from 95.1% to 105.2%, with relative standard deviations (RSD) of 3.4% to 8.5%, providing a new technical approach for the rapid on-site detection of antibiotic residues.

References

[1] TAKAHASHI Y, IGARASHI M. Destination of aminoglycoside antibiotics in the 'post-antibiotic era' [J]. J Antibiot, 2018, 71(1): 4-14.

[2] YAGI K, ISHII M, NAMKOONG H, et al. The efficacy, safety, and feasibility of inhaled amikacin for the treatment of difficult-to-treat non-tuberculous mycobacterial lung diseases [J]. BMC Infect Dis, 2017, 17(9.

[3] ZHANG X P, WANG J J, WU Q H, et al. Determination of Kanamycin by High Performance Liquid Chromatography [J]. Molecules, 2019, 24(10): 24.

[4] YU S J, WEI Q, DU B, et al. Label-free immunosensor for the detection of kanamycin using Ag@Fe3O4 nanoparticles and thionine mixed graphene sheet [J]. Biosens Bioelectron, 2013, 48(224-9.

[5] CHEN B, ZHANG H, LIN B, et al. Determination of streptomycin residue in cucumber and chinese cabbage by high-performance liquid chromatography with postcolumn derivatization and fluorometric detection [J]. 2012, 95(2): 523-7.

[6] KITASATO I, YOKOTA M, INOUYE S, et al. Comparative ototoxicity of ribostamycin, dactimicin, dibekacin, kanamycin, amikacin, tobramycin, gentamicin, sisomicin and netilmicin in the inner ear of guinea pigs [J]. 1990, 36(2): 155-68.

[7] LIU B, ZHANG B, CUI Y, et al. Multifunctional gold–silica nanostructures for ultrasensitive electrochemical immunoassay of streptomycin residues [J]. 2011, 3(12): 4668-76.

[8] LIAO Q G, WEI B H, LUO L G. Aptamer based fluorometric determination of kanamycin using double-stranded DNA and carbon nanotubes [J]. Microchim Acta, 2017, 184(2): 627-32.

[9] JI Y X, HUANG Y, CHENG Z H, et al. Lateral Flow Strip Biosensors for Foodborne Pathogenic Bacteria via Direct and Indirect Sensing Strategies: A Review [J]. J Agric Food Chem, 2023, 71(27): 10250-68.

[10] HUANG L J, SUN D W, PU H B, et al. Development of Nanozymes for Food Quality and Safety Detection: Principles and Recent Applications [J]. Compr Rev Food Sci Food Saf, 2019, 18(5): 1496-513.

[11] BANTI M J I J O N, SCIENCES F. Food adulteration and some methods of detection, review [J]. 2020, 9(3): 86-94.

[12] XU Y, CHEN L, WANG X C, et al. Recent advances in noble metal based composite nanocatalysts: colloidal synthesis, properties, and catalytic applications [J]. Nanoscale, 2015, 7(24): 10559-83.

[13] XIONG H X, HU P P, ZHANG M M, et al. Recent advances of nanozyme-enhanced lateral flow assay sensing in clinic diagnosis [J]. Microchem J, 2024, 206(18.

[14] LIU J, ZENG J Y, TIAN Y P, et al. An aptamer and functionalized nanoparticle-based strip biosensor for on-site detection of kanamycin in food samples [J]. Analyst, 2018, 143(1): 182-9.

[15] TOH S Y, CITARTAN M, GOPINATH S C B, et al. Aptamers as a replacement for antibodies in enzyme-linked immunosorbent assay [J]. Biosens Bioelectron, 2015, 64(392-403.

[16] LOYNACHAN C N, THOMAS M R, GRAY E R, et al. Platinum Nanocatalyst Amplification: Redefining the Gold Standard for Lateral Flow Immunoassays with Ultrabroad Dynamic Range [J]. ACS Nano, 2018, 12(1): 279-88.

[17] ROMIH T, JEMEC A, KOS M, et al. The role of PVP in the bioavailability of Ag from the PVP-stabilized Ag nanoparticle suspension [J]. Environ Pollut, 2016, 218(957-64.

[18] ZHAN L, GUO S Z, SONG F Y, et al. The Role of Nanoparticle Design in Determining Analytical Performance of Lateral Flow Immunoassays [J]. Nano Lett, 2017, 17(12): 7207-12.

[19] SMIRNOV M Y, KALINKIN A V, VOVK E I, et al. Analysis of the oxidation state of platinum particles in supported catalysts by double differentiation of XPS lines [J]. J Struct Chem, 2016, 57(6): 1127-33.

[20] PANFEROV V G, WANG X Q, LIU J W. Characterization of nanozyme kinetics for highly sensitive detection [J]. Analyst, 2024, 149(8): 2223-6.

[21] GAO L, ZHUANG J, NIE L, et al. Intrinsic peroxidase-like activity of ferromagnetic nanoparticles [J]. 2007, 2(9): 577-83.

[22] PEREIRA A E S, SILVA P M, OLIVEIRA J L, et al. Chitosan nanoparticles as carrier systems for the plant growth hormone gibberellic acid [J]. Colloid Surf B-Biointerfaces, 2017, 150(141-52.

[23] UEMURA N, EGOSHI T, MURAKAMI K, et al. High-power laser irradiation for high-temperature in situ transmission electron microscopy [J]. Micron, 2022, 157(13.

[24] ZHU X, TANG J, OUYANG X L, et al. A versatile CuCo@PDA nanozyme-based aptamer-mediated lateral flow assay for highly sensitive, on-site and dual-readout detection of Aflatoxin B1 [J]. J Hazard Mater, 2024, 465(9.

[25] BEAVEN G H, HOLIDAY E R. ULTRAVIOLET ABSORPTION SPECTRA OF PROTEINS AND AMINO ACIDS [J]. AdvProtein Chem, 1952, 7(319-86.

[26] SOLTANI S, OJAGHI A, ROBLES F E. Deep UV dispersion and absorption spectroscopy of biomolecules [J]. Biomed Opt Express, 2019, 10(2): 487-99.

[27] YANG Z, YI C, LV S J, et al. Development of a lateral flow strip biosensor based on copper oxide nanoparticles for rapid and sensitive detection of HPV16 DNA [J]. Sens Actuator B-Chem, 2019, 285(326-32.